

DESY-SR 72/15
September 1972

DESY-Bibliothek
3. NOV. 1972

Photoabsorption of Atomic Sodium in the VUV

by

H.W. Wolff, K. Radler, B. Sonntag, and R. Haensel

II. Institut für Experimentalphysik der Universität Hamburg, Hamburg, Germany

and

Deutsches Elektronen-Synchrotron DESY, Hamburg, Germany

To be sure that your preprints
are promptly included in the
HIGH ENERGY PHYSICS INDEX, send
them to the following address
(if possible by air mail):

DESY
Bibliothek
2 Hamburg 52
Notkestieg 1
Germany

Photoabsorption of Atomic Sodium in the VUV

H.W. Wolff, K. Radler, B. Sonntag, and R. Haensel

II. Institut für Experimentalphysik der Universität Hamburg, Hamburg, Germany

and

Deutsches Elektronen-Synchrotron DESY, Hamburg, Germany

The absorption spectrum of atomic sodium in the photon energy region from 30 eV to 150 eV has been investigated. A great number of sharp absorption lines which can be attributed to the excitation of a 2p- or a 2s-electron has been detected. Simultaneous excitation of one 2p- and one 3s-electron gives rise to considerably strong broad and asymmetric absorption structures above the highest series limit (1P_1) for the excitations of a single 2p-electron. Some of the assignments have been confirmed by Hartree-Fock calculations. The relative spectral dependence of the absorption cross-section in this energy range has been determined for the first time. The spectrum of free Na atoms has been compared with the $L_{II,III}$ spectrum of solid sodium.

I. INTRODUCTION

The sharp lines showing up in absorption spectra at the onset of inner shell transitions of free atoms give detailed information on the electron states. This information has in many cases also turned out to be of great use for the interpretation of the absorption spectra of solids formed by these atoms¹. In this respect the atomic absorption spectra due to transitions of the tightly bound core electrons to continuum states can also be very helpful. The investigation of the 2p-absorption of atomic sodium has been initiated by absorption measurements on the simple metals Na, Mg and Al². The L_{II,III} absorption spectra of these metals show broad periodic structures up to 100 eV above threshold. These structures cannot be explained in terms of the one-electron band model. Lundqvist et al.^{3,4} have tried to interpret these maxima with the help of the so-called "plasmaron theory" which demands simultaneous excitation of collective modes and the core electron. This theory correctly describes the position of these peaks for Al; it fails, however, to give the positions of these peaks for Na and Mg.

Absorption measurements in the VUV showed that the continuum absorption of many solids is very similar to that of the corresponding free atoms¹. Most of the absorption spectra can be understood, at least qualitatively, in terms of a one-electron model for free atoms⁵. Taking into account, however, multiplet splitting, configuration interaction and electron-correlation Dehmer et al.^{6,7} and Amusia et al.⁸ achieved quantitative agreement between their calculations and the experimental results.

Calculations⁹ of the photoionization cross-section for the 2p-absorption of atomic Na, Mg and Al in terms of a one-electron model only give one broad maximum above the onset of the 2p-absorption. Atomic data, on the other hand, indicate that transitions from the 2s-states and simultaneous excitations of one 2p-electron and one 3s-electron or two 2p-electrons respectively might be responsible for at least part of the structures detected in the 2p-absorption spectra of these simple metals. As there were no measurements of the 2p-continuum absorption of atomic Na available we measured the 2p absorption of sodium vapour in the energy region from 30 eV to 150 eV. One major object of these measurements was to find out how closely the 2p-absorption of solid sodium resembled the 2p-spectrum of atomic sodium and whether the periodic structures mentioned above were due to solid state effects.

II. EXPERIMENTAL PROCEDURE

The 7.5 GeV electron synchrotron DESY served as a continuum background source^{10,11}. The fine structure at the onset of the 2p-transitions of sodium was measured with a 2 m grazing incidence Rowland spectrograph (McPherson Model 247). The spectra were recorded on photographic plates (Kodak SWR, Ilford Q2). Two different aluminum coated gratings were used, one with 600 lines/mm and one with 1,200 lines/mm. The blaze angle was $2^{\circ}4'$ for both gratings. Measurements at an angle of incidence of $82^{\circ}30'$ and of $84^{\circ}30'$ were performed. The resolution achieved was better than 0.08 \AA with the 1,200 lines/mm grating and better than 0.15 \AA with the 600 lines/mm grating over the entire energy region. The exposure times varied between some minutes and several hours depending on the electron current in the accelerator, the pressure conditions in the sodium vapour furnace and the thickness and materials of the windows used for confining the vapour.

In order to avoid the tedious and difficult task of calibrating the intensity response of the photographic plates the spectral dependence of the absorption cross-section was measured with a 1 m grazing incidence Rowland spectrometer. In this case an open magnetic type multiplier (Bendix M 306), mounted behind the exit slit was used as a detector. A gold coated grating with 2,400 lines/mm and a blaze angle of $4^{\circ}16'$ with an angle of incidence of $77^{\circ}14'$ was used. Because of the high absorption of the sodium vapour we had to open the entrance slit and, as a result, the wavelength resolution was limited to 0.2 \AA over the measured energy range. Details of the experimental set-up and the experimental procedure are given in Refs. 11,12. The spectrometer was calibrated by the known He resonance lines¹³. The He resonance lines and some very sharp absorption

lines of atomic Na determined by Connerade et al.¹⁴ were used for the wavelength calibration of the photographic plates.

The sodium vapour furnace using the heat pipe principle¹⁵ was mounted in front of the spectrographs. A buffer gas of helium prevented the sodium from reaching the aluminum, magnesium or zapon windows which confined the vapour region. The thickness of the windows ranged from 500 Å to 1,000 Å. They were supported by a 75 µm copper mesh. These windows also served as filters suppressing higher orders reflected from the grating. We additionally used Si prefilters in the energy region from 70 eV to 100 eV. The sodium vapour pressures varied from 0.1 Torr up to 0.5 Torr (temperature up to 410° C). The temperature profile along the stainless steel furnace was measured by thermocouples. The absorption path length was 40 to 70 cm. As the spectrum of the synchrotron radiation is completely smooth and continuous, any structure found in the spectra can, with a high degree of reliability, be attributed to the sodium vapour. The well-known structures due to the absorption of the windows and the He buffer gas could easily be separated from the structures due to the sodium vapour.

III. EXPERIMENTAL RESULTS

The absorption spectrum of sodium vapour in the measured energy region is shown by the solid line in Fig. 1. Since the temperature profile along the furnace and consequently the pressure and the length of the sodium vapour column could not be determined very exactly only the relative shape of the absorption spectrum was measured. The absorption spectrum shown in Fig. 1 has been adjusted to the absolute cross-section calculated by McGuire⁹ (dotted curve). The same holds for the absorption spectrum of solid Na² given by the dashed curve. As for atomic sodium no absolute cross-sections have been determined for solid sodium. Under the conditions of our measurements the percentage of Na₂ molecules is expected to be about 3 %¹⁶. Though the absorption due to this molecular contribution is expected to be small compared to the absorption due to Na atoms we cannot exclude that some of the weak structures showing up in the spectra are due to Na₂ molecules. Careful study of the temperature dependence of the spectra over a considerable temperature range might help to clarify this question but these experiments still remain to be done.

At the onset of transitions from the 2p-shell of atomic sodium we find two strong sharp lines. The background due to transitions of the outer 3s-electron seems to be almost exhausted in this energy region⁹. Apart from some broader and weaker structures a considerable number of sharp lines show up in the spectrum towards higher energies. The appearance of these lines changes abruptly above 38.5 eV. Above this energy the spectrum is dominated by relatively broad and asymmetric structures. These structures could be detected up to 47 eV. Above 47 eV the absorption cross-section increases smoothly. Between 65 and 71 eV transitions from the 2s-level give

rise to prominent, broad and asymmetric absorption lines. Towards still higher energies the cross-section decreases smoothly. Up to 150 eV no further structures could be detected.

Part of this spectrum has already been reported by Connerade et al.¹⁴. Probably due to a lower vapour pressure, lower intensity of the BRV source used in these measurements and the difficulties caused by the line structure already present in the spectrum emitted by the source, Connerade et al. have only been able to detect the strongest lines in the energy range up to 50 eV. Only the first strong line at 66 eV due to the excitation of the 2s-electrons has shown up in their measurements. Simultaneous to our measurements Ederer et al.¹⁷ measured the absorption of atomic sodium using synchrotron radiation. According to preliminary results there seems to be good agreement between their results and ours in the energy region up to 50 eV. They have not examined the structures between 65 eV and 71 eV.

The relative spectral dependence of the absorption coefficient between 30 eV and 150 eV has been determined by our measurements using photoelectric detection for the first time.

IV. DISCUSSION

For the purpose of discussion the measured absorption spectrum (Fig. 1) will be divided into four parts. In part A the overall behaviour of the measured absorption spectrum will be discussed and compared to the absorption spectrum of solid sodium² and to the results of McGuire's³ calculations for free sodium atoms. Part B deals with the absorption lines in the energy range from 30 eV to 38.5 eV being due to transitions from the 2p-shell of atomic Na. The double excitations giving rise to the structures between 38.5 eV and 50 eV will be discussed in part C. Transitions from the 2s-shell showing up between 65 eV and 72 eV will be treated in part D.

A. Continuum Absorption

McGuire³ has calculated the photoionization cross-section for atomic sodium by a one-electron model using the atomic potential tabulated by Herman and Skillman¹¹. The dotted line in Fig. 1 gives the results of these calculations. The onset of the transitions of the Na 2p-electrons into continuum states given by McGuire lies about 4 eV below the experimentally determined energy position of the lowest series limits $^3P_{2,1,2}$, 1P_1 . (3P_2 37.986 eV, 1P_1 38.081 eV, 3P_0 38.155 eV, 3P_1 38.462 eV, these energies have been obtained by adding the ionization energy of Na to the energy of the lowest excited states of Na^+ , all values taken from the tables by C.E. Moore¹².) Both theory and experiment show a considerable increase in the absorption cross-section at threshold. Above this threshold the absorption cross-section increases giving rise to a broad maximum at about 60 eV. Towards still higher energies the absorption decreases. This general feature is shown by both the theoretical and the experimental curve. The broad maximum can be explained in terms of a one-electron model for free atoms as being

due to the delayed onset of transitions⁵ from the 2p-states to d-symmetric final states. A potential barrier at the edge of the atom depresses these transitions at threshold and shifts the oscillator strength towards higher energies. Transitions to bound final states are not included in McGuire's calculations. The sharp absorption lines and the prominent structures due to double excitations are, therefore, not to be found in the theoretical curve. The onset of the transitions from the 2s-states of Na to continuum states given by the calculations also lies at about 4 eV below the series limits $2s2p^63s \ ^3S_1, \ ^1S_0$. Again the structures found experimentally between 65 eV and 71 eV are not reproduced by the calculations.

The absorption spectrum of solid sodium given by the dashed line in Fig. 1 also shows a broad maximum at about 60 eV. Three prominent maxima are superimposed at 48.5 eV, 65.5 eV and 90 eV. Similar maxima have been detected in the 2p-absorption spectra of solid Mg, Al² and Si²⁰. These maxima cannot be explained by one-electron band models. They might as has already been pointed out^{3,4} be due to the simultaneous excitation of one 2p-electron and one, two, or three plasmons. By coupling the plasmon to the 2p-core hole the energy of the plasmon is shifted to higher energies as compared to the energy of the normal bulk mode.

From atomic data¹⁹ and from the results of Hartree-Fock calculations²¹ one can estimate the highest series limit for the simultaneous excitation of one 2p-electron and one 3s-electron to be at about 53 eV, for the excitation of one 2s-electron at 72 eV, and for the simultaneous excitation of two 2p-electrons at about 110 eV. This means that these series limits approximately coincide with the high energy tail of the three maxima found in the absorption spectra of solid sodium. The same holds for the 2p-

absorption spectra of solid Mg and Al. Part of these three maxima might, therefore, be due to these excitations. However, no maxima show up in the spectrum of sodium vapour at the energy where we find the first and the third maximum in the solid. Only at the position of the second maximum around 65 eV do we find strong absorption structures in the spectrum of sodium vapour being due to 2s-transitions. These structures might be broadened when going from the free atoms to the solid and at least part of this peak might, therefore, be due to 2s-excitations. All this leads to the conclusion that these three maxima cannot be explained by atomic excitations alone. Solid state effects seem to be very important. At present a convincing explanation for those maxima has not, as yet, been given.

B. Region from 30 eV to 38.5 eV

At the onset of the 2p-transitions two strong lines show up at 30.768 eV and at 30.934 eV. These lines are due to the transitions $2p^6 3s \ ^2S_{1/2} \rightarrow 2p^5 3s \ ^2P_{1/2, 3/2}$ of atomic sodium. The energy positions of these lines are very close to the position of the L_{III} (30.68 ± 0.1 eV) and L_{II} (30.84 ± 0.1 eV) edges in solid sodium. The value of the spin orbit splitting (0.16 eV) agrees well with the result of Hartree-Fock²¹ calculations for free sodium atoms and with the energy separation of the L_{III} and the L_{II} edge found for solid sodium. The structures detected between 31 eV and 35 eV cannot be explained by atomic excitations and are possibly due to excitations of Na_2 molecules.

The lines experimentally determined in the region up to 38.5 eV are tabulated together with a tentative interpretation in Tables I and II.

The lines above 35 eV are shown on an enlarged scale in Fig. 2. These lines are due to following type of transitions:

$$2p^4 3s \ ^1S_{1/2} \rightarrow 2p^4 3s n s \quad n \geq 4$$

$$2p^4 3s n d \quad n \geq 3$$

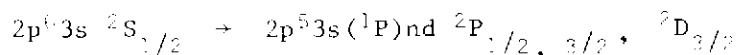
Taking into account the selection rules for dipole allowed transitions there are 17 series converging to the series limits $2p^4 3s \ ^3P_{2,1,0}, \ ^1P_1$. It is impossible to pick out series by eye below the 3P_1 series limit because of the complicated experimental spectrum due to the great number of overlapping series. Connerade et al.¹⁷ calculated the effective quantum number for all the lines detected by them and thereby obtained a tentative assignment of the lines. Because of the great number of very closely spaced lines and the effect of interaction between overlapping configurations which has to be taken into account, we question the reliability of assignments based on this procedure. Furthermore, the strength and the appearance of the lines do not lead to an unambiguous identification.

By diagonalizing the energy matrices we calculated the energy position and the relative oscillator strength of the lines belonging to the $2p^4 3s 4s$ and the $2p^4 3s 3d$ configuration of atomic sodium. These matrices have been obtained with the help of the tables given by Slater²² and by Condon and Shortley²³. Furthermore, the energy matrices obtained in this way have been checked using the graphical tensor operator techniques given by Briggs²⁴ and the code developed by Hibbert²⁵. The pertinent values for the Coulomb, exchange and spin-orbit energies have been calculated by the Hartree-Fock code developed by Froese Fischer²¹. These two configurations should correspond to the lines found in the spectrum up to 36.7 eV. The results of the calculations are included in Fig. 2. The center of

gravity of the calculated configurations has been adjusted to the experimental results. No adjustment has been applied to the splitting of the lines calculated for one configuration. Between the calculated energy splitting and the experimental results we find reasonable agreement for the four lines with lowest energy. Furthermore, the relative oscillator strengths calculated for these lines are in reasonable agreement with those determined experimentally. Towards higher energies there are considerable differences between the calculated and the experimental spectrum. This might be due to the interaction between the $2p^6 3s 4s$ configuration and the overlapping $2p^5 3s 3d$ configuration. We have not taken configuration interaction into account in our calculations.

Similar calculations have been made for the configurations $2p^6 3s n s$ and $2p^6 3s n d$ with n up to 15. Because of the complexity of the spectra no unambiguous correlation between the results of these calculations and the experimental results could be found. The interaction between the overlapping configurations seems to modify the spectrum considerably. In order, therefore, to give a reliable interpretation calculations taking into account the interactions between all overlapping configurations have to be performed. We have not tried to tackle this extensive task.

Above the 2P_0 series limit series converging to the 1P_1 series limit can be seen clearly. The energy position of these lines and their interpretation are listed in Table II. The strong, broader lines are due to the following transitions:



These lines seem to be broadened by the interaction with the underlying continuum. The different levels could, therefore, not be resolved. The

sharp weaker lines are due to the transitions

$$2p^6 3s \ ^2S_{1/2} \rightarrow 2p^5 3s ({}^1P) ns \ ^2P_{1/2, 3/2}$$

The interaction of these lines with the underlying continuum seems to be smaller. This can be concluded from the narrow line width which, in some cases, even permitted us to separate both components.

C. Region from 38.5 eV to 50 eV

Above the 1P_1 series limit simultaneous excitations of a 2p-electron and a 3s-electron give rise to broad asymmetric structures extending up to 47 eV. These structures are shown on an enlarged scale in Fig. 3. According to the selection rules the following dipole transitions can take place.

$$\begin{array}{lll}
 2p^6 3s & \rightarrow & 2p^5 ns n' s & n, n' \geq 4 \\
 & & 2p^5 ns n' d & n \geq 4 \quad n' \geq 3 \\
 & & 2p^5 np n' p & n, n' \geq 3 \\
 & & 2p^5 nd n' d & n, n' \geq 3 \\
 & & 2p^5 np n' f & n \geq 3 \quad n' \geq 4
 \end{array}$$

Because of the large number of overlapping series converging to excited states of the Na^+ ion the interpretation of this part of the spectrum seems to be very difficult. Part of the lower lying series limits taken from C.E. Moore's tables⁽¹⁾ are included in Fig. 3. There seems to be considerable interaction between the overlapping series and between the series and the underlying continua which gives rise to a broadening of the structures. The interaction of the series with the underlying continua also gives rise to asymmetric and window-type lines. One series of window-type lines converging

towards the $2p^5(^2P_{1/2})3p^3S_1$ level of Na^{+19} can easily be picked out by eye. There seems to be another series converging to the $2p^5(^2P_{1/2})3p^1S_0$ level of Na^{+19} . The spectrum becomes even more complicated towards higher energies due to the increasing number of series. According to atomic data¹⁹ the high energy limit of these double excitations should be at 52.612 eV which corresponds to the energy position of the $2s^22p^5$ states of Na^{++} . The spectrum becomes smooth already at 47 eV.

D. Region from 65 eV to 72 eV

Transitions from the 2s-level give rise to the strong asymmetric lines found in the energy region between 65 eV and 72 eV. These lines are shown on an enlarged scale in Fig. 4. According to Hartree-Fock calculations the onset of the simultaneous excitation of two 2p-electrons or the simultaneous excitation of one 2s- and one 3s-electron should lie above 73 eV. We do not, therefore, have to take these double excitations in the energy range under consideration into account. Consequently, in the following we will concentrate on transitions of the type:



These transitions should give rise to series converging to the $2s2p^63s^3S_1$ and $2s2p^63s^1S_0$ level of Na^+ . Hartree-Fock calculations place the center of this configuration between 70 eV and 72 eV. The energy splitting between the 3S_1 and the 1S_0 states is expected to be about 0.9 eV. The energy position of the $2s2p^63s$ configuration of Na^+ can also be estimated from atomic data¹⁹. The $2s2p^6$ configuration of Na^{++} lies 85.2 eV above the ground state of Na. The binding energy of the 3s-electron in the $2s2p^63s$ configuration of Na^+ should be very close to the binding energy of the 3s-electron in the state

$2s^2 2p^6 3s$ of Mg^+ , thus replacing the Na^+ $2s$ hole by a proton inside the Mg^+ nucleus. By subtracting this binding energy of 15 eV from 85.2 eV we end up with an energy of 70.2 eV which is in agreement with the results of the Hartree-Fock calculations.

Hartree-Fock calculations for the $2s2p^6 3s3p$ and the $2s2p^6 3s4p$ configurations of sodium, taking into account oscillator strengths, lead to the assignment of the strong line at 66.6 eV to the $2s2p^6 3s ({}^3S) 3p {}^2P$ states and to the assignment of the line at 69.6 eV to the $2s2p^6 3s ({}^3S) 4p {}^2P$ states. These lines are highly asymmetric indicating a considerable interaction with the underlying continua. We tried, therefore, to fit these lines by profiles represented by the formula

$$\sigma(\epsilon) = \sigma_a \frac{(q+\epsilon)^2}{(1+\epsilon)^2} + \sigma_b$$

$$\epsilon = (E-E_r)/\frac{1}{2}\Gamma$$

given by U. Fano and J.W. Cooper²⁵. Here ϵ gives the departure of the incident photon energy E from the resonance energy E_r . This departure is expressed in a scale whose unit is the half-width $\frac{1}{2}\Gamma$ of the line. $\sigma(\epsilon)$ represents the absorption cross-section for photon energy E whereas σ_a and σ_b represent two portions of the cross-section corresponding, respectively, to transitions to states of the continuum which do and do not interact with the discrete state. q is a numerical index which characterizes the line profile. These relations hold for the interaction of one discrete line with one continuum.

The calculated profiles, giving the best fit to the experimental data, are shown by the dashed curves in Fig. 4. The parameter q we used was -2 for the line at 66.6 eV and -1.8 for the line at 69.6 eV. A value -1.6 for the q parameter has also been found for the auto-ionizing $2s\ 2p^5 \rightarrow 2s2p^4 3p$ line in Ne^{+7} , which is next to Na in the periodic table. The shoulder at 66 eV might be due to the $2s2p^6 3s$ (3S) $3p$ 4P states. The maximum at 68 eV has been assigned to the $2s2p^6 3s$ (1S) $3p$ 2P states. The suggested energy positions of the 3S and 1S series limits are indicated by bars in Fig. 4. The splitting of the LS terms due to the spin orbit interaction is not expected to show up in the spectrum due to the small value of the spin orbit parameter ($\zeta_{3p} \approx 0.004$ eV, $\zeta_{4p} \approx 0.0005$ eV)¹¹.

Acknowledgment

The authors would like to thank the Deutsche Forschungsgemeinschaft for financial support.

References

1. see e.g. R. Haensel and B. Sonntag, in Computational Solid State Physics, ed. F. Herman, N.W. Dalton, Th.R. Koehler (Plenum Press New York - London 1972) p. 43 and references therein
2. R. Haensel, G. Keitel, B. Sonntag, C. Kunz, and P. Schreiber, *phys.stat.sol. (a)* 2, 85 (1970)
3. L. Hedin and S. Lundqvist, in Solid State Physics, Vol. 23, ed. F. Seitz, D. Turnbull, H. Ehrenreich (Academic Press, New York and London 1969)p. 1
4. B.I. Lundqvist, Thesis, Chalmers Univ. of Technol., Göteborg 1969
5. U. Fano and J.W. Cooper, *Rev.Mod.Phys.* 40, 441 (1968)
6. J.L. Dehmer, A.F. Starace, U. Fano, J. Sugar and J.W. Cooper, *Phys. Rev. Letters* 26, 1521 (1971)
7. J.L. Dehmer and A.F. Starace, *Phys.Rev.* B5, 1792 (1972)
8. M.Y. Amusia, N.A. Cherepkov, and L.V. Chernysheva, *Soviet Physics JETP* 33, 90 (1971)
9. E.J. McGuire, Research Report SC-RR-721 Sandia Laboratories (1970)
10. R. Haensel and C. Kunz, *Z. Angew. Phys.* 23, 276 (1967)
11. R.P. Godwin, in Springer Tracts in Modern Physics, Vol. 51, ed. G. Hühler (Springer Verlag, Berlin 1969)p. 1
12. P. Rabe, B. Sonntag, T. Sagawa, and R. Haensel, *phys.stat.sol. (b)* 50, 559 (1972)
13. R.P. Madden and K. Codling, *Astrophys. J.* 141, 364 (1965)
14. J.P. Connerade, W.R.S. Garton and M.W.D. Mansfield, *Astrophys. J.* 165, 203 (1971)
15. C.R. Vidal and J. Cooper, *J.Appl.Phys.* 40, 3370 (1969)
16. A.N. Nesmeyanov, Vapor Pressure of the Chemical Elements, ed. R. Gary (Elsevier Publishing Company, Amsterdam, London, New York 1963) p. 423

17. D.L. Ederer private communication
see also:
D.L. Ederer, T. Lucatorto and R.P. Madden, paper given at the
III. International Conference on Vacuum Ultraviolet Radiation
Physics, Tokyo 1971 (unpublished)
18. F. Herman and S. Skillman, Atomic Structure Calculations (Prentice
Hall, Inc. Englewood Cliffs, N.J. 1963)
19. C.E. Moore, Natl. Bur. Std. (U.S.) Circ. No 467 (U.S. GPO Washington,
D.C.) Vol. I (1949)
20. Ch. Gähwiler and F.C. Brown, Phys.Rev. B 2, 1918 (1970)
21. for the Hartree-Fock calculations we used a code developed by
C. Froese Fischer. C. Froese Fischer, Computer Phys. Comm. 1,
151 (1969)
22. J.C. Slater, Quantum Theory of Atomic Structure (McGraw Hill Book
Co. New York, 1960)
23. E.U. Condon and G.H. Shortley, The Theory of Atomic Spectra
(Cambridge at the University Press 1970)
24. J.S. Briggs, Rev.Mod.Phys. 43, 189 (1971)
25. A. Hibbert, Computer Phys. Comm. 1, 359 (1969)
26. U. Fano and J.W. Cooper, Phys.Rev. 137, A 1364 (1965)
27. K. Codling, R.P. Madden and D.L. Ederer, Phys.Rev. 155, 26 (1967)

Table Captions

Table I Observed 2p-electron excitation up to the $2p^5 3s \ ^3P_{2,1,0}$ ionization limits¹⁹. Identified transitions are given in column 5. The assignments for the lines above 35.8 eV are less reliable than those for the lines at lower energy because of the differences between the calculated energy positions and oscillator strengths and the experimental results (see chapter IV B and Fig. 2). "C" denotes the lines previously published in Ref. 14.

Table II Series of lines converging to the $2p^5 3s \ ^2P_1$ ionization limit¹⁹. The effective quantum number n^* is given in column 5. "C" denotes the lines previously published in Ref. 14.

Figure Captions

- Fig. 1 Spectral dependence of the absorption cross-section of atomic sodium (solid line) and solid sodium² (dashed line) in the energy range 30 - 150 eV given in arbitrary units. For comparison the absolute cross-sections calculated by McGuire⁹ are included (dotted line).
- Fig. 2 Absorption of atomic sodium in the energy range 35 - 39 eV. Since in the photoelectric measurements not all line structure found in this energy range could be resolved, the relative oscillator strengths of the absorption lines has been obtained by taking into account both the photoelectric and the photographic measurements. Most of the absorption lines are due to transitions of the type $2p^63s \rightarrow 2p^53sns$ and $2p^63s \rightarrow 2p^53snd$. The energy positions of the series limits are taken from Ref. 19. The calculated energy splittings and relative oscillator strengths of the lines of the $2p^52s4s$ and $2p^53s3d$ configurations are included.
- Fig. 3 Absorption spectrum of atomic sodium in the energy range 38.5 - 46.5 eV. The structure is due to the simultaneous excitation of one 2p- and one 3s-electron. The energy position of the ten lowest series limits, all of them belonging to the $2p^53p$ configuration of the Na^+ ion, have been taken from Ref. 19.

Fig. 4 Absorption lines due to 2s-electron excitation. The series limits have been obtained from Hartree-Fock calculations. The best fit of the data by a Fano profile¹¹ is given by the dashed curves.

Table I

λ (\AA)	$h\nu$ (eV)	Appearance			Assignment
402.97	30.768		broad, very	strong	C $1s^2 2s^2 2p^5 3s^2 \ ^2P_{3/2}$
400.80	30.934		broad, very	strong	C $1s^2 2s^2 2p^5 3s^2 \ ^2P_{1/2}$
394.6	31.42	very	broad,	strong	molecular abs.
392.6	31.58	very	broad,	strong	molecular abs.
363.30	34.128		broad,	weak	
359.71	34.468		broad,	weak	
358.05	34.628		broad,	weak	
353.44	35.080	very	broad,	weak	
351.69	35.254	very	broad,	weak	
350.22	35.402	very	broad,	weak	
348.61	35.566	fairly	broad,	weak	$2p^5 3s(3P)4s \ ^4P_{3/2}$
347.97	35.631	fairly	broad,	weak	$2p^5 3s(3P)4s \ ^4P_{1/2}$
346.64	35.768		broad,	strong	C $2p^5 3s(3P)4s \ ^2P_{3/2}$
346.42	35.790	fairly	broad, fairly	strong	C $2p^5 3s(3P)4s \ ^2P_{1/2}$
346.07	35.827	fairly	broad,	weak	$2p^5 3s(3P)3d \ ^4P_{3/2}$
345.83	35.852	fairly	broad,	weak	$2p^5 3s(3P)3d \ ^4P_{1/2}$
344.55	35.985		broad, very	strong	C $2p^5 3s(3P)3d$
344.23	36.018	fairly	broad,	strong	C $2p^5 3s(3P)3d$
343.87	36.056		broad,	strong	C $2p^5 3s(3P)3d$
343.49	36.096	fairly	broad, very	weak	
343.17	36.129	fairly	broad,	strong	C $2p^5 3s(3P)3d$
342.34	36.217		broad,	strong	C
342.10	36.242		sharp, very	weak	
341.28	36.330		sharp, very	weak	
341.19	36.339		sharp, very	weak	
340.68	36.394		sharp, very	weak	
338.62	36.615		sharp, fairly	strong	C
338.36	36.643		sharp,	weak	C
338.11	36.670		sharp, very	weak	
336.61	36.834	fairly	broad,	weak	
335.95	36.906		broad, very	strong	C $2p^5 3s(3P)4d$
335.74	36.929	fairly	broad,	strong	C $2p^5 3s(3P)4d$
335.18	36.991	fairly	broad,	weak	
334.46	37.070	fairly	broad,	strong	$2p^5 3s(3P)4d$
333.98	37.124		sharp, very	weak	

λ (Å)	hν (eV)	Appearance	Assignment
332.64	37.273	fairly broad, fairly strong	C 2p ³ 3s(³ P)5d
332.47	37.292	fairly broad, fairly strong	C 2p ³ 3s(³ P)5d
332.27	37.315	sharp, very weak	
331.76	37.372	sharp, weak	
331.69	37.380	sharp, weak	
331.58	37.392	sharp, very weak	
331.15	37.441	fairly broad, fairly strong	C 2p ³ 3s(³ P)5d
330.98	37.460	sharp, weak	C
330.65	37.497	fairly broad, fairly strong	C
330.37	37.529	sharp, very weak	
330.24	37.544	sharp, weak	C
330.10	37.560	sharp, very weak	
329.78	37.596	sharp, weak	C
329.70	37.606	sharp, very weak	
329.58	37.619	sharp, very weak	C
329.47	37.632	sharp, very weak	
329.37	37.643	sharp, very weak	
329.24	37.658	sharp, very weak	C
329.07	37.678	sharp, very weak	
328.97	37.689	sharp, very weak	
328.94	37.692	sharp, very weak	
328.88	37.699	fairly broad, strong	C
328.57	37.735	sharp, very weak	
328.46	37.747	sharp, very weak	
328.35	37.760	fairly broad, strong	C
328.22	37.775	sharp, very weak	
328.13	37.785	sharp, weak	C
328.00	37.800	fairly broad, fairly strong	C
327.93	37.808	sharp, very weak	
327.82	37.821	sharp, very weak	
327.70	37.835	sharp, very weak	
327.64	37.842	sharp, fairly strong	C
327.53	37.855	sharp, very weak	
327.44	37.865	fairly broad, strong	C
327.28	37.884	sharp, weak	
327.16	37.897	sharp, fairly strong	C
327.06	37.909	sharp, very weak	

λ (\AA)	$h\nu$ (eV)	Appearance	Assignment
326.98	37.918	sharp,	weak
326.91	37.926	sharp,	weak
326.85	37.933	sharp,	weak
326.75	37.945	sharp, very	weak
326.63	37.959	sharp, very	weak
326.53	37.971	fairly broad,	weak
326.34	37.993	broad,	strong C
326.25	38.003	sharp, very	weak
326.12	38.018	sharp, very	weak
326.40	37.986		$2p^5 3s(^3P_2)$
325.58	38.081		$(^3P_1)$
324.95	38.155		$(^3P_0)$
			limits

Table II

λ (Å)	$h\nu$ (eV)	Appearance	n^*	Assignment
325.85	38.050	broad, very strong C	5.74	$2p^5 3s(1P_1) 6d$
325.21	38.125	fairly broad, fairly strong C	6.35	$(1P_1) 8s \quad 4P$
324.90	38.161	broad, very strong C	6.72	$(1P_1) 7d$
324.53	38.205	fairly broad, weak C	7.27	$(1P_1) 9s \quad 2P$
324.30	38.232	broad, strong C	7.68	$(1P_1) 8d$
324.08	38.258	sharp, very weak	8.15	$(1P_1) 10s \quad 2P_{3/2}$
324.02	38.265	sharp, very weak	8.30	$(1P_1) 10s \quad 2P_{1/2}$
323.90	38.279	fairly broad, strong C	8.61	$(1P_1) 9d$
323.74	38.298	sharp, very weak	9.10	$(1P_1) 11s \quad 2P_{3/2}$
323.69	38.304	sharp, very weak	9.26	$(1P_1) 11s \quad 2P_{1/2}$
323.60	38.314	fairly broad, fairly strong C	9.59	$(1P_1) 10d$
323.46	38.331	sharp, very weak	10.18	$(1P_1) 12s$
323.39	38.339	fairly broad, fairly strong C	10.51	$(1P_1) 11d$
323.23	38.358	fairly broad, weak C	11.44	$(1P_1) 12d$
323.11	38.373	fairly broad, weak	12.31	$(1P_1) 13d$
323.01	38.384	sharp, weak	13.22	$(1P_1) 14d$
322.94	38.393	sharp, very weak	13.98	$(1P_1) 15d$
322.88	38.400	sharp, very weak	14.76	$(1P_1) 16d$
322.83	38.406	sharp, very weak	15.52	$(1P_1) 17d$
322.79	38.411	sharp, very weak	16.22	$(1P_1) 18d$
322.75	38.415	sharp, very weak	17.02	$(1P_1) 19d$
322.72	38.419	sharp, very weak	17.70	$(1P_1) 20d$
322.36	38.461			$2p^5 3s(1P_1)$ limit

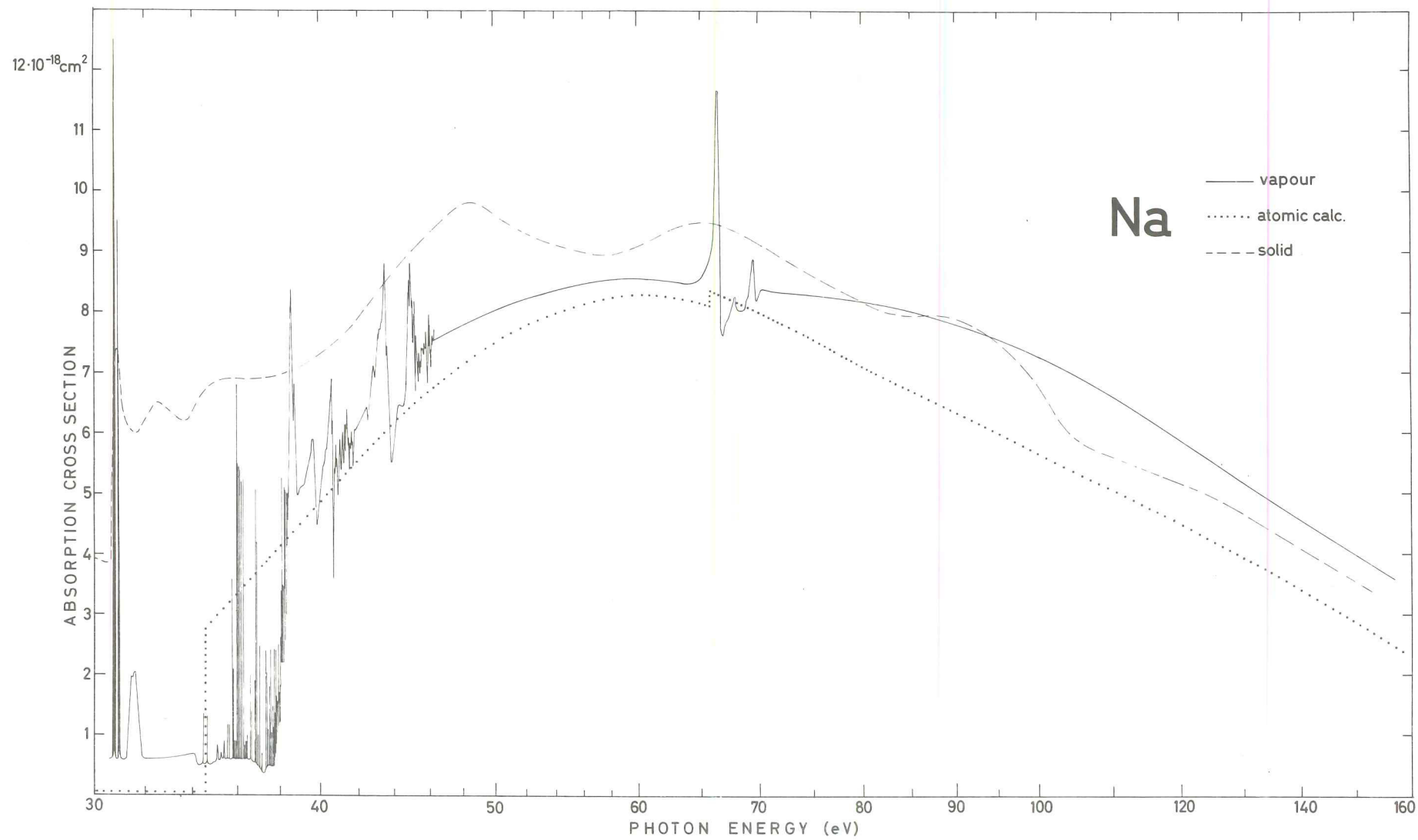


Fig. 1

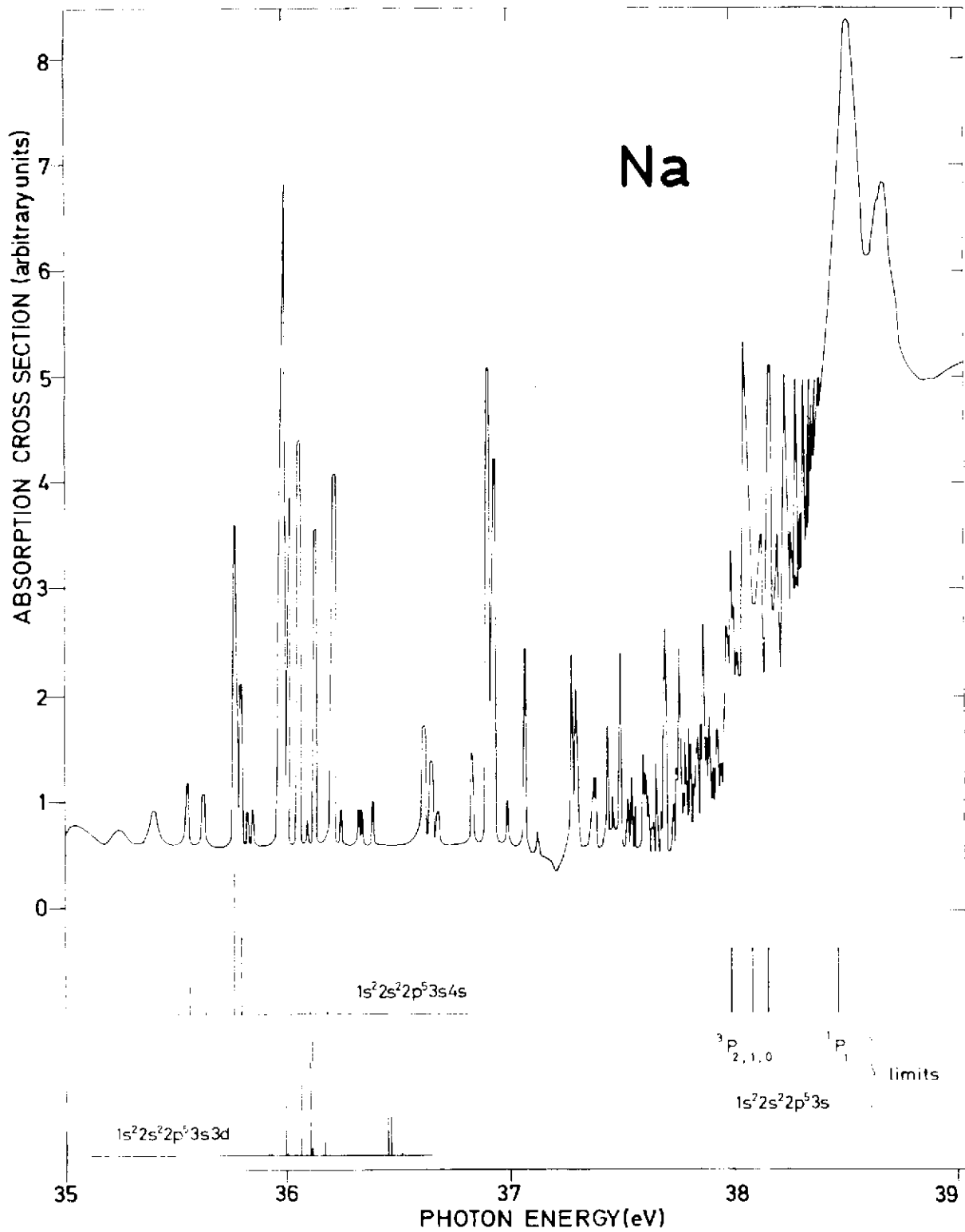


Fig. 2

